Received September 5, 2019, accepted September 17, 2019, date of publication September 27, 2019,
date of current version October 16, 2019.

Digital Object Identifier 10.1109/ACCESS.2019.2944233

An Equivalent Aggregated Model of Large-Scale Flexible Loads for Load Scheduling

JING TU[1,2], (Student Member, IEEE), MING ZHOU[1], (Member, IEEE), HANTAO CUI[2], (Member, IEEE), AND FANGXING LI[2], (Fellow, IEEE)

[1]State Key Laboratory of Alternate Electrical Power System with Renewable Energy Sources, North China Electric Power University, Beijing 102206, China
[2]Department of Electrical Engineering and Computer Science, The University of Tennessee, Knoxville, TN 37996, USA

Corresponding author: Ming Zhou (zhouming@ncepu.edu.cn)

This work was supported in part by the National Natural Science Foundation of China under Grant U1866204 and Grant 51577061, in part by the National Key Research and Development Program under Grant 2016YFB0901100, and in part by the China Scholarship Council under Grant 201806730056.

ABSTRACT The popularity of smart applications enables the large-scale integration of flexible loads to power systems, which poses a considerable challenge to system scheduling. Focusing on scheduling optimization with large-scale flexible loads, this paper proposes the equivalent aggregated method for flexible loads, which converts a large number of flexible loads into a few equivalent models to participate in system scheduling. In order to establish the equivalent model, flexible loads are grouped based on their parameters such that loads with the same or similar parameters are clustered into the same group. Then, the equivalent model for each group is established, a proof of the equivalence relationship between the original model and the equivalent model is provided, and the upper bound of equivalence deviations is estimated. The whole equivalent aggregated model is expressed as the sum of equivalent models of all groups. Afterwards, a new approach of applying the equivalent aggregated model to system scheduling is proposed. Case studies show that the equivalent aggregated model can effectively schedule large-scale flexible loads to shave the peak and fill the valley, with small equivalent deviations and fast calculation speed. This validates the proposed model and demonstrates its promising applications to large-scale load scheduling.

INDEX TERMS Load modeling, optimal scheduling, load management, smart grids.

NOMENCLATURE

SET

Ω	Set of all flexible loads
$\mathcal{P}_i$	Set of all feasible power of flexible load i
$\mathcal{P}_g$	Set of all feasible power of group g
$\mathcal{P}_{g,e}$	Set of all feasible power of the equivalent model of group g
$\mathcal{P}_r$	Set of all feasible power of the relaxation model
$\mathcal{U}$	Set of all flexible loads in the Unclassified Group

INDICES

i, N	Index and number of flexible loads
t, T	Index and number of time intervals.
g, M	Index and number of groups, except the Unclassified Group

PARAMETERS

Δt	The duration of a time interval (h)
ε	Small non-negative integer
P_i^{rate}	Rated power of flexible load i (kW)
E_i	Required energy of flexible load i (kW · h)
T_i	Necessary work intervals of flexible load i
α_i	Start time of the schedulable period for flexible load i
β_i	End time of the schedulable period for flexible load i
P_g^{rate}	Rated power of flexible loads in group g (kW)
α_g	Start time of the schedulable period for flexible loads in group g
β_g	End time of the schedulable period for flexible loads in group g
T_g	Necessary work intervals for flexible loads in group g

VARIABLES

$P_i(t)$	Power of flexible load i at time t (kW)

The associate editor coordinating the review of this manuscript and approving it for publication was Yang Li.

$u_i(t)$	Binary variable for the operating state of ON/OFF flexible load i at time t
$P_g(t)$	Power of group g at time t (kW)
$P_{g,e}(t)$	Power of the equivalent model of group g at time t (kW)
$P_\Omega(t)$	Power of set Ω at time t (kW)
$P_r(t)$	Power of the relaxation model at time t (kW)
$P_i(\cdot)$	Power vector composed of $P_i(t)$ at all times (kW)
$P_g(\cdot)$	Power vector composed of $P_g(t)$ at all times (kW)
$P_{g,e}(\cdot)$	Power vector composed of $P_{g,e}(t)$ at all times (kW)
$P_\Omega(\cdot)$	Power vector composed of $P_\Omega(t)$ at all times (kW)
$P_r(\cdot)$	Power vector composed of $P_r(t)$ at all times (kW)

I. INTRODUCTION

With the development of the smart grid and the popularity of smart applications in residential, commercial, and industrial loads, controllable flexible loads have been connected to power systems in large amounts, bringing flexibility as well as challenges to power system operations [1]. Based on market prices or control signals of the system operator, flexible loads can shift power usage from peak to valley, thereby reducing the peak load and the operating cost of a power system [2]. The flexibility of loads also enables power system operators to integrate more renewable energy [3].

Currently, two types of flexible loads are widely studied: 1) thermostatically controlled loads represented by air conditioners, and 2) interruptible & shiftable loads represented by electric vehicles. On the one hand, because of the thermal inertia, the thermostatically controlled load is suitable for short-term power adjustment. Hence relevant research mainly focuses on frequency regulation [4]–[6], reserve services [7], and so on. On the other hand, the interruptible & shiftable load is able to flexibly arrange the operating power within a large period of time [8], cutting the peak load and filling the valley [9], which makes it more suitable for day-ahead and intraday scheduling. This paper therefore takes the interruptible & shiftable load as the research objective for scheduling, and it is referred to as the flexible load in the rest of this paper.

Centralized scheduling with large flexible loads is hard to solve in a limited time by conventional algorithms, because hundreds of millions of variables and constraints are introduced into the scheduling formulation by these loads. Therefore, it is necessary to seek new models and methods to solve scheduling optimization with large-scale flexible loads. Generally, there are two solutions for large-scale problems. The first one is to apply distributed computation techniques to solve large-scale problems through distributed models and algorithms. The second is to apply the aggregated models, which aggregate a large number of flexible loads into a smaller number of aggregated load models. By narrowing the scale of the problem, the model can be solved by conventional algorithms.

In distributed computing research, distributed control is widely applied in the scheduling of the micro-gird [10], [11], and for scheduling with larger-scale flexible loads, the distributed algorithms based on the alternating direction method of multipliers and game theory are verified to be effective. Rivera *et al.* [12] formulated a versatile and scalable distributed convex optimization framework, which in simulation scheduled a million flexible loads to fill system valleys within 30 minutes. For multiperiod optimal power flow optimization with flexible loads, Fan *et al.* [13] developed a distributed algorithm based on alternating direction method of multipliers, updating steps by alternating iterations. The scalability and effectiveness of the algorithm is also tested. Mohsenian-Rad *et al.* [14] presented an autonomous and distributed demand-side energy management system among users through game theory and proved the optimality and convergence of the model when the power of the loads is continuous. De Paola *et al.* [15] extended the work in [14], coordinating the continuous or ON/OFF loads operating in the electricity market with the framework of game theory. A distributed iterative algorithm based on Nash equilibrium is designed and tested with the large-scale loads. Kumar *et al.* [16] proposed an aggregative game for flexible loads in the day-ahead electricity market, and tested with 100,000 loads; however, the calculation time was not illustrated. Chen and Cheng [17] applied game theory to aggregating a large number of users to provide operational reserves to the power system through load aggregators. In addition, the impact of communication on distributed computing has also been studied [18], [19].

In research on aggregated models, the bi-level optimization model has been widely applied, and the grouping scheduling method has also been developed. In the upper level of the bi-level model, a group of flexible loads are aggregated into a certain model, such as the aggregate battery model [20], which then participates in the day-ahead scheduling or electricity market [21]. In the lower level, the individual models of the flexible loads are used to fit the group power obtained in the upper level [22]. Li *et al.* [23] modeled a group of batteries as an aggregate battery and used it to participate in the power balance of the micro-grid. Wang *et al.* [24] applied an aggregated battery to model a group of flexible loads. They first scheduled the battery power at the time-of-use price to achieve a minimum cost, and then disaggregated the power to each individual load. Khan *et al.* [25] designed the interaction process between the distribution system operator and the aggregators; then the aggregators used a water injection algorithm in the two-step disaggregation of load power to reduce the disaggregation deviations. As a special type of bi-level model, the grouping scheduling method first groups flexible loads according to their characteristics [26], and then establishes an aggregation model for each group to participate in the scheduling of the upper model. Shi *et al.* [27] applied charging time and arrival time as grouping criteria.

The electric vehicles with similar parameters were clustered in a group, and then participated in the scheduling of the micro-grid. Huang *et al.* [28] used schedulable time period and charging time to group the loads, and interval optimization was applied to build the upper model. Pan *et al.* [29] extended the work in [28], distributing the power of flexible loads in a group in proportion to their required electricity. However, this distribution method cannot be used for ON/OFF loads.

In the above research, although the distributed algorithms can solve scheduling with large-scale flexible loads, the current fast-distributed algorithms also need tens of minutes to complete the optimization [12], [15]. In addition, there may be certain communication problems. For the bi-level scheduling model, although the flexible loads are expressed as an aggregated model in the upper level, since the established aggregated model is not an equivalent model, it is necessary to use the lower level to fit the power of the aggregated model. Although the grouping scheduling thought is proposed, the equivalence of the group model has not been proved [26]–[29], and the disaggregation deviations cannot be estimated in advance. Furthermore, there is a lack of adaptive analysis for large-scale load scheduling. To address this deficiency, this paper 1) proposes an equivalent aggregated model of flexible loads based on grouping equivalence, 2) proves the equivalence of the aggregated model and the upper bound of the equivalence deviations, and 3) establishes a corresponding scheduling method for large-scale flexible loads. The main contributions of this paper are as follows:

- Based on grouping equivalence, an equivalent aggregated method for large-scale flexible loads is proposed. Due to the diversity of the parameters of flexible loads, it is difficult to directly establish an equivalent model for all flexible loads. Hence, this paper clusters flexible loads with the same or similar parameters into a group and establishes an equivalent model for each group. Then the whole equivalent aggregated model can be expressed as the sum of equivalent models of all groups.
- The equivalent model for a single group of flexible loads with the same or similar parameters is proposed. For continuous flexible loads and ON/OFF flexible loads, their linear continuous equivalent models are established respectively, which are approximate to hydropower plant models. Then the equivalence relationship between the models is proved and the equivalence deviations are estimated.
- A method of applying the equivalent aggregated model to the scheduling process is proposed. For scheduling with large-scale flexible loads, all the steps of applying the equivalent aggregated model are discussed in detail, including the criteria for grouping, the grouping process, optimization and power disaggregation of the equivalent model.

The rest of the paper is organized as follows: The mathematical model of individual flexible loads and the classification criteria of groups are presented in Section II. Section III presents the definition of the equivalent model, establishes the equivalent model for a single group of flexible loads and estimates the equivalence deviations. Section IV describes the method of scheduling with the equivalent aggregated model. Section V presents and discusses a case study of the proposed model. Section VI follows with conclusions.

II. EQUIVALENCE AGGREGATED METHOD FOR LARGE-SCALE FLEXIBLE LOADS

In this section, we first present the individual and aggregated models of the flexible loads, and then propose an equivalence method to build an equivalent aggregated model based on grouping.

A. MODEL OF FLEXIBLE LOADS

The flexible load studied in this paper is the load that can flexibly adjust its power consumption in a certain period of time, while the total energy consumed is fixed. According to power adjustment modes, flexible loads can be classified as continuous loads and ON/OFF loads. The former can continuously adjust its power consumption, whereas the latter can only control power through ON/OFF.

In order to schedule flexible loads, a day is divided into T equal time intervals. As for a flexible load i with P_i^{rate} and E_i, we can calculate T_i by $T_i = E_i/(P_i^{rate}\Delta t)$, and then use T_i instead of E_i as its parameter.

For a continuous flexible load i with schedulable period $[\alpha_i, \beta_i]$, P_i^{rate} and T_i, its individual model is as follows [30]:

$$0 \le P_i(t) \le P_i^{rate}, \quad \forall t \in [\alpha_i, \beta_i] \tag{1}$$

$$P_i(t) = 0, \quad \forall t \notin [\alpha_i, \beta_i] \tag{2}$$

$$\sum_{t\in[\alpha_i,\beta_i]} P_i(t) = T_i P_i^{rate} \tag{3}$$

$$\mathcal{P}_i = \{P_i(\cdot)\,|P_i(t) \text{ subject to } (1)-(3)\} \tag{4}$$

Equations (1-2) ensure that flexible load i only works during its schedulable period and its power does not exceed its rated power. Equation (3) ensures its working time is enough.

If the flexible load i is an ON/OFF load, its individual model is:

$$P_i(t) = u_i(t)P_i^{rate}, \quad u_i(t) \in \{0, 1\}, \ \forall t \in [\alpha_i, \beta_i] \tag{5}$$

$$\mathcal{P}_i = \{P_i(\cdot)\,|P_i(t) \text{ subject to } (2), (3), (5)\} \tag{6}$$

For the ON/OFF load, the T_i needs to be an integer to ensure $\mathcal{P}_i \neq \emptyset$. Therefore, we assume that each T_i appearing in this paper is a positive integer, whether for a continuous load or an ON/OFF load.

Afterwards, the aggregated model of flexible loads is established based on the individual models. For a set Ω including millions of flexible loads, its power should be equal to the sum of the power of all flexible loads in the set:

$$\mathcal{P}_\Omega = \left\{ P_\Omega(\cdot) \,\middle|\, P_\Omega(\cdot) = \sum_{i\in\Omega} P_i(\cdot),\ P_i(\cdot) \in \mathcal{P}_i \right\} \tag{7}$$

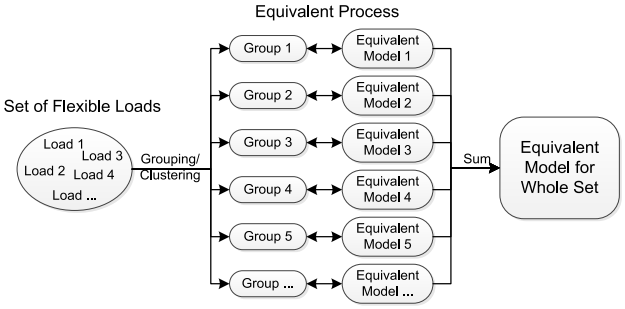

FIGURE 1. Process of grouping equivalence.

Then for the power of set Ω, $P_\Omega(t)$, there should be:

$$P_\Omega(t) = \sum_{i\in\Omega} P_i(t), \quad \forall t \tag{8}$$

B. GROUPING EQUIVALENCE

Computational complexity increases rapidly with the size of the problem, leading to the need for an equivalent model. As for a set of flexible loads as described by (7), there could be hundreds of millions of variables and constraints in the aggregated model, creating problems for load scheduling. Therefore, we hope to find the equivalent model. However, due to the diversity of the parameters of flexible loads, it is difficult to use a simple mathematical model to equate the aggregated model. Hence, a method of grouping equivalence is proposed to solve it.

The key to grouping equivalence is clustering flexible loads of the same or similar parameters into a group, and then establishing an equivalent model for each group. In this way, the aggregated model for a set of flexible loads is equivalent to the sum of the equivalent models of all groups. Fig.1 illustrates this process.

The criteria for grouping are the parameters of flexible loads. According to the individual model, the parameters of flexible load i are P_i^{rate}, α_i, β_i, and T_i, by which the flexible loads can be divided into groups. For a set of flexible loads, some typical values are selected from the distributions of P_i^{rate}, α_i, β_i, and T_i, as the grouping criteria. These typical values are used as the ranges of the groups' parameters. By combining these typical values in the ranges, a series of groups with different parameters are generated. Then each load is sorted into the group whose parameters are closest to its parameters. After grouping, the loads in each group have the same or similar parameters. Then the equivalent model for a group is established, as discussed in the next section.

III. EQUIVALENT MODEL FOR A SINGLE GROUP

This section presents the equivalent model for a group of flexible loads with the same or similar parameters. First, the mathematical definition of the equivalent model is described by set theory. Then the equivalent models of the groups with continuous loads or ON/OFF loads are established. Finally, we analyze how to merge groups and establish the equivalent model for a merged group.

A. DEFINITION OF THE EQUIVALENT MODEL

The equivalent model is established when the loads in a group are thought of as a whole as far as their total power is concerned. Then a model that has the same total power can replace the group; this is the equivalent model. Because the total power of the group is actually a feasible domain, the equivalence means the two models have the same feasible domain of the total power. Therefore, the equivalent model can be defined by set theory as follows:

Definition 1: For load model A, B of the following form:

Load A:

$$\mathcal{P}_A = \{P_A(\cdot) \mid H_A(P_A(\cdot), Y_A) = 0,\ G_A(P_A(\cdot), Y_A) \le 0\} \tag{9}$$

Load B:

$$\mathcal{P}_B = \{P_B(\cdot) \mid H_B(P_B(\cdot), Y_B) = 0,\ G_B(P_B(\cdot), Y_B) \le 0\} \tag{10}$$

If $\mathcal{P}_B = \mathcal{P}_A$, then load model B is called the equivalent model of load model A, and load model B is said to be equivalent to load model A.

where $P_{\mathrm{A}}(\cdot)$, $P_{\mathrm{B}}(\cdot)$ is the total power vector of load model A, B; $\mathcal{P}_{\mathrm{A}}$, $\mathcal{P}_{\mathrm{B}}$ is the set of all feasible power vectors $P_{\mathrm{A}}(\cdot)$, $P_{\mathrm{B}}(\cdot)$; H_{A}, H_{B} are the equality constraints of load model A, B, and G_{A}, G_{B} are the inequality constraints; and Y_{A}, Y_{B} are the variables in constraints except $P_{\mathrm{A}}(\cdot)$, $P_{\mathrm{B}}(\cdot)$.

In Definition 1, the equivalence relationship between load models is symmetrical. If B is equivalent to A, A must be equivalent to B.

However, the equivalence relationship in Definition 1 is so strict that it allows for no deviation in equivalence, which may lead to difficulties in establishing the equivalent model. However, an equivalent model with a small deviation is actually acceptable. Hence, an equivalence relationship with a certain deviation is proposed as follows:

Definition 2: Consider load model A, B of the form in (9-10). Their feasible domains of total power are $\mathcal{P}_{\mathrm{A}}$ and $\mathcal{P}_{\mathrm{B}}$. If for some $\varepsilon \ge 0$ the following condition (11-12) is fulfilled:

$$\forall x \in \mathcal{P}_A, \quad \exists y \in P_B, \ \|y - x\| \le \varepsilon \tag{11}$$

$$\forall y \in P_B, \quad \exists x \in P_A, \ \|x - y\| \le \varepsilon \tag{12}$$

Then load model B is called the ε-equivalent model of load model A, and load model B is said to be ε-equivalent to load model A.

The ε-equivalence relationship is also symmetrical. If $\varepsilon = 0$, the ε-equivalence will turn into an equivalence relationship in Definition 1, which indicates that Definition 2 is an extension of Definition 1. In addition, the $\|\cdot\|_\infty$ is used for Definition 2 in this paper, because it represents the upper limit of absolute deviations at all times.

B. EQUIVALENT MODEL FOR CONTINUOUS LOADS

For a group of N continuous flexible loads with the same parameters, the equivalent model is established by the following theorem:

Theorem 1: For a group of N continuous flexible loads with the same parameters of P_g^{rate}, α_g, β_g, and T_g, the model $\mathcal{P}_g$ is in the following form:

$$\mathcal{P}_g = \left\{ P_g(\cdot) \left| \begin{array}{c} P_g(t) = \sum_{i=1}^{N} P_i(t),\ \forall t \\ 0 \le P_i(t) \le P_g^{rate},\ \forall i,\ \forall t \\ P_i(t) = 0,\ t \notin [\alpha_g, \beta_g],\ \forall i \\ \sum_t P_i(t) = T_g P_g^{rate},\ \forall i \end{array} \right. \right\} \tag{13}$$

The model $\mathcal{P}_g$ could be equivalent to the model $\mathcal{P}_{g,e}$, whose form is as follows:

$$\mathcal{P}_{g,e} = \left\{ P_{g,e}(\cdot) \left| \begin{array}{c} 0 \le P_{g,e}(t) \le N P_g^{rate},\ \forall t \\ P_{g,e}(t) = 0,\ t \notin [\alpha_g, \beta_g] \\ \sum_t P_{g,e}(t) = N T_g P_g^{rate} \end{array} \right. \right\} \tag{14}$$

Proof: According to Definition 1, $\mathcal{P}_g$ is equivalent to the model $\mathcal{P}_{g,e}$, meaning:

$$\mathcal{P}_g = \mathcal{P}_{g,e} \tag{15}$$

Proving (15) is equivalent to proving (16) & (17):

$$\forall P_g(\cdot) \in \mathcal{P}_g, \quad \exists P_{g,e}(\cdot) = P_g(\cdot),\ P_{g,e}(\cdot) \in P_{g,e} \tag{16}$$

$$\forall P_{g,e}(\cdot) \in P_{g,e}, \quad \exists P_g(\cdot) = P_{g,e}(\cdot),\ P_g(\cdot) \in P_g \tag{17}$$

① To prove (16), we can sum the constraints for $P_i(t)$ in $\mathcal{P}_g$, and then the constraints for $P_g(t)$ can be obtained. The constraints for $P_g(t)$ are the same as the constraints in $\mathcal{P}_{g,e}$. Hence, for any $P_g(\cdot) \in \mathcal{P}_g$, let the $P_{g,e}(\cdot) = P_g(\cdot)$, and the $P_{g,e}(\cdot)$ must fulfill the constraints in $\mathcal{P}_{g,e}$, so there is always $P_g(\cdot) = P_{g,e}(\cdot) \in \mathcal{P}_{g,e}$. Equation (16) is fulfilled.

② To prove (17), for any $P_{g,e}(t)$ in $\mathcal{P}_{g,e}$, we can let every $P_i(t)$ be equal to $P_{g,e}(t)/N$. It's easy to verify that every $P_i(t)$ satisfies the constraints in $\mathcal{P}_g$. Therefore, for $P_g(\cdot)$ that is the sum of these $P_i(t)$, there is $P_g(\cdot) \in \mathcal{P}_g$. Meanwhile, $P_g(\cdot) = P_{g,e}(\cdot)$. Equation (17) is fulfilled.

Theorem 1 is thereby verified, and establishes an accurate equivalent model for continuous loads. The model has linear constraints on energy and power, which makes it approximate to a hydropower plant model.

C. EQUIVALENT MODEL FOR ON/OFF LOADS

The equivalent model for ON/OFF flexible loads has a wider range of applications. Loads with continuously adjustable power usually need to be controlled by electronic power devices, whereas the ON/OFF loads can be controlled with cheaper and simpler smart switches. Continuous loads can also operate in ON/OFF mode, indicating that the equivalent model for ON/OFF loads can be applied to continuous loads.

1) DISCRETE EQUIVALENT MODEL

For a group of N ON/OFF flexible loads with the same parameters, a discrete equivalent model is established by the following theorem:

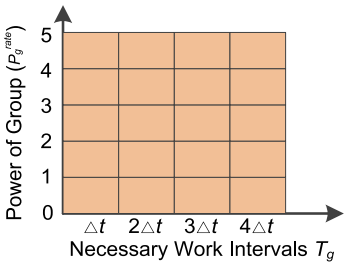

FIGURE 2. Energy of ON/OFF flexible loads for operation.

Theorem 2: For a group of N ON/OFF flexible loads with the same parameters of P_g^{rate}, α_g, β_g, and T_g, if its model $\mathcal{P}_g$ is in the following form:

$$\mathcal{P}_g = \left\{ P_g(\cdot) \left| \begin{array}{c} P_g(t) = \sum_{i=1}^{N} P_i(t),\ \forall t \\ P_i(t) = u_i(t) P_g^{rate},\ \forall t,\ \forall i \\ u_i(t) \in \{0, 1\},\ \forall t, \forall i \\ P_i(t) = 0,\ t \notin [\alpha_g, \beta_g],\ \forall i \\ \sum_t P_i(t) = T_g P_g^{rate},\ \forall i \end{array} \right. \right\} \tag{18}$$

Then the model $\mathcal{P}_g$ could be equivalent to the model $\mathcal{P}_{g,e}$ with a discrete power range, whose form is as follows:

$$\mathcal{P}_{g,e} = \left\{ P_{g,e}(\cdot) \left| \begin{array}{c} P_{g,e}(t) \in \{0, P_g^{rate}, 2P_g^{rate}, 3P_g^{rate}, \cdots, NP_g^{rate}\} \\ P_{g,e}(t) = 0,\ t \notin [\alpha_g, \beta_g] \\ \sum_t P_{g,e}(t) = N T_g P_g^{rate} \end{array} \right. \right\} \tag{19}$$

Proof: $\mathcal{P}_g$ being equivalent to the model $\mathcal{P}_{g,e}$ means (16) and (17) are fulfilled.

Just like the proof in Theorem 1, Equation (16) is easy to verify by summing the constraints for $P_i(t)$ in $\mathcal{P}_g$. Therefore, we focus on the proof of (17).

The key to proving (17) is that for any $P_{g,e}(\cdot)$ in $\mathcal{P}_{g,e}$, if there is an algorithm that can always find a $P_g(\cdot)$ that belongs to $\mathcal{P}_g$ and is equal to $P_{g,e}(\cdot)$, Equation (17) must be fulfilled. To find the $P_g(\cdot)$, the main function of the algorithm is to disaggregate the $P_{g,e}(\cdot)$ into the sum of the $P_i(t)$ with their constraints fulfilled. If it is possible, the $P_g(\cdot)$, as the sum of the $P_i(t)$ must belong to $\mathcal{P}_g$ and be equal to $P_{g,e}(\cdot)$. Algorithm 1 is thus proposed to disaggregate the $P_{g,e}(\cdot)$ into the sum of the $P_i(t)$.

Algorithm 1: Power Disaggregation Algorithm for Discrete Equivalent Model

First, the group of ON/OFF loads and $P_{g,e}(\cdot) \in \mathcal{P}_{g,e}$ are described. For a group of N ON/OFF loads with the same parameters of P_g^{rate}, α_g, β_g, and T_g, the energy that the group of loads need for working is described by Fig.2.

In Theorem 2, N and T_g can be any positive integers, and in Fig.2, $N = 5$ and $T_g = 4$, are used as the example integers to illustrate Algorithm 1. The horizontal axis represents necessary work intervals for loads in the group, and they are the

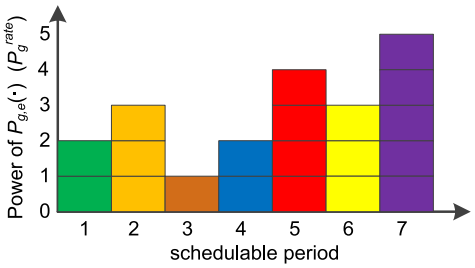

FIGURE 3. A power curve of the discrete equivalent model.

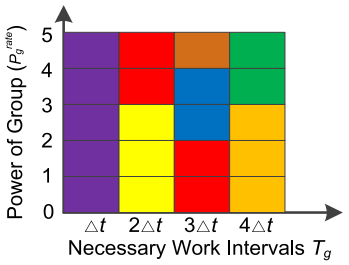

FIGURE 4. Result of allocation from power curve of the discrete equivalent model to energy of ON /OFF flexible loads.

same as T_g. based on conditions of Theorem 2. The vertical axis represents the power of the group, with the unit of P_g^{rate}. Energy blocks of all loads are shown in Fig.2, and each row of blocks represents the energy used by one load.

The $P_{g,e}(\cdot) \in \mathcal{P}_{g,e}$ can be described in Fig.3, as an illustrative example of Algorithm 1.

In Fig.3, the horizontal axis represents schedulable time intervals, and the vertical axis represents the power of the $P_{g,e}(\cdot)$. The $P_{g,e}(\cdot)$ has the same energy as in Fig.2, and its power is discrete and no more than NP_g^{rate}. For clarity, energy blocks at each time are marked with a unique color.

In order to find the $P_g(\cdot)$ that fulfills (17), the objective of Algorithm 1 is to allocate energy blocks in Fig.3 to Fig.2 in an operational way for loads, meaning that the allocation must fulfill the constraints for the loads. Since the numbers of energy blocks in Fig.3 and Fig.2 are the same, after allocation, the number of energy blocks allocated to each load is T_g; hence (3) is always fulfilled. Since the power of each load is 0 or P_g^{rate}, this requires that energy blocks at a certain time cannot be allocated to a load with more than one block. If the allocation is completed, then the $P_i(t)$ for every load can be found, and the $P_g(\cdot) = P_{g,e}(\cdot)$ can be found.

Allocation steps in Algorithm 1 are as follows:

① Choose the energy blocks of a time that has not been allocated in Fig.3.

② Start the allocation in Fig.2 from the first unallocated column of energy blocks on the right side of the figure, in order from top to bottom. If the column is partly allocated, start the allocation from the top of the unallocated energy blocks of the column. If energy blocks in this column are all allocated during the allocation, turn to the left column next to this column and continue allocation from top to bottom.

Repeat steps one and two until all of the energy blocks in Fig.3 are allocated. Because the numbers of energy blocks in Fig.2 and Fig.3 are the same, the allocation will be finished in Fig.2 and Fig.3 at the same time. The result of allocation is shown in Fig.4. Then Algorithm 1 is finished.

It's easy to verify that in Algorithm 1, energy blocks at a certain time are not allocated to a load with more than one block. In Algorithm 1, allocation is carried out from right to left and from top to bottom. In this order of allocation, only when $P_{g,e}(t)$ is greater than NP_g^{rate}, will there be a load obtaining two energy blocks of $P_{g,e}(t)$. However in (19) $P_{g,e}(t)$ can never be greater than NP_g^{rate}, which ensures a load will not obtain more than one energy block of $P_{g,e}(t)$ at a certain time; therefore the allocation is operational.

Thus, Equation (17) in Theorem 2 is verified by Algorithm 1, and then Theorem 2 is verified.

Theorem 2 establishes an accurate equivalent model for ON/OFF loads, and hence reveals their flexibility. The Theorem indicates that even if the flexible loads can only work in ON/OFF mode, a group of loads with the same parameters can work like a hydropower plant model with a discrete power range, which means the group of ON/OFF loads and the hydropower plant have similar flexibility.

2) CONTINUOUS EQUIVALENT MODEL

Through the ε-equivalence in Definition 2, a continuous equivalent model for ON/OFF flexible loads is established by the following Theorem:

Theorem 3: For a group of N ON/OFF flexible loads with the same parameters of P_g^{rate}, α_g, β_g, and T_g, if its model $\mathcal{P}_g$is in the form of (18), there is a model $\mathcal{P}_{g,e}$ that is ε-equivalent to $\mathcal{P}_g$, and in ε-equivalence, the $\|\cdot\| = \|\cdot\|_\infty$ and $\varepsilon = P_g^{rate}$. The form of $\mathcal{P}_{g,e}$ is (14).

Proof: $\mathcal{P}_{g,e}$ ε-equivalent to the model $\mathcal{P}_g$ means:

$$\forall P_g(\cdot) \in P_g, \quad \exists P_{g,e}(\cdot) \in P_{g,e}, \quad \left\|P_{g,e}(\cdot) - P_g(\cdot)\right\|_\infty \leq \varepsilon = P_g^{rate} \tag{20}$$

$$\forall P_{g,e}(\cdot) \in P_{g,e}, \quad \exists P_g(\cdot) \in P_g, \quad \left\|P_g(\cdot) - P_{g,e}(\cdot)\right\|_\infty \leq \varepsilon = P_g^{rate} \tag{21}$$

For (20), it's obvious that $\mathcal{P}_g \subseteq \mathcal{P}_{g,e}$, hence:

$$\forall P_g(\cdot) \in P_g, \quad \exists P_{g,e}(\cdot) \in P_{g,e}, \quad P_{g,e}(\cdot) = P_g(\cdot) \tag{22}$$

$$\therefore \left\|P_{g,e}(\cdot) - P_g(\cdot)\right\|_\infty = 0 \leq \varepsilon = P_g^{rate} \tag{23}$$

Therefore, Equation (20) is verified.

The key to proving (21) is the same as in Theorem 2, which is to propose an algorithm that can always find the $P_g(\cdot)$ which fulfills (21). In order to find the $P_g(\cdot)$, Algorithm 2, as an extension of Algorithm1, is proposed as follows.

Algorithm 2: Power Disaggregation Algorithm for Continuous Equivalent Model

First the group of ON/OFF loads and the $P_{g,e}(\cdot) \in \mathcal{P}_{g,e}$ need to be described. In Theorem 3, the group of ON/OFF loads is

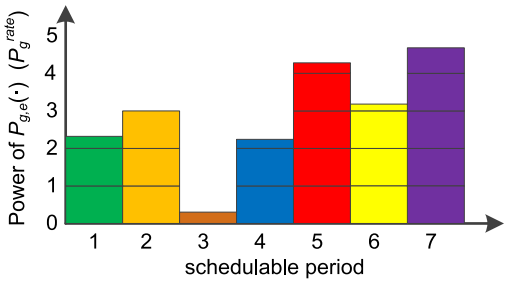

FIGURE 5. A power curve of the continuous equivalent model.

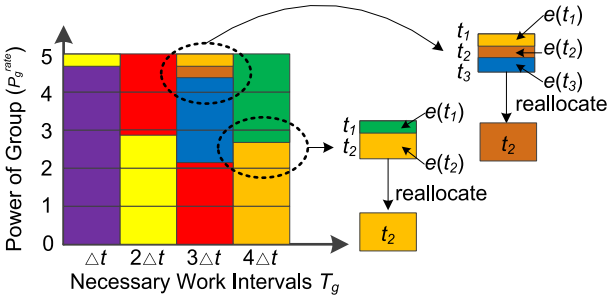

FIGURE 6. Allocation and reallocation from power curve of continuous equivalent model to energy of ON /OFF flexible loads.

the same as that in Theorem 2, so the energy they need is also described by Fig.2. The $P_{g,e}(\cdot) \in \mathcal{P}_{g,e}$ can be described in Fig.5. The $P_{g,e}(\cdot)$ in Fig.5 has the same energy as Fig.2, but its power range is a continuous interval $[0, NP_g^{rate}]$.

Allocation steps in Algorithm 2 are as follows:

① Choose the energy blocks of a certain time that has not been allocated in Fig.5.

② Start the allocation for Fig.2 from right to left and from top to bottom. Because $P_{g,e}(t)$ is a real number, there will be an energy block in Fig.2 partly occupied by $P_{g,e}(t)$. The next allocation starts from an unoccupied part of this energy block. The results of allocation are shown in Fig.6.

Some energy blocks in Fig.6 have more than one color, representing the need for loads to operate at different times with partial power of P_g^{rate}, which is inoperable for an ON/OFF load. Therefore, the next step is to reallocate these energy blocks to one of the $P_{g,e}(t)$ that occupy it.

③ Reallocate the energy blocks that have more than one color based on the following rules:

Rule A: If the energy block has two colors, from top to bottom, record the times corresponding to these two colors as t_1, t_2; the energy they occupy in the energy block is recorded as $e(t_1)$, $e(t_2)$. If $e(t_1) \geq 0.5\ P_g^{rate}\Delta t$, the energy block is reallocated to t_1, otherwise the energy block is reallocated to t_2. $P_g^{rate}\Delta t$ is the energy of this block.

Rule B: If the energy block has K colors, $K \geq 3$, from top to bottom, record the times corresponding to these K colors as $t_1, t_2, \ldots, t_{K-1}, t_K$; and record the energy they occupy in the energy block as $e(t_1), e(t_2), \ldots, e(t_{K-1}), e(t_K)$. If $e(t_1) \geq 0.5P_g^{rate}\Delta t$, the energy block is reallocated to t_1. Otherwise, if $e(t_K) > 0.5P_g^{rate}\Delta t$, the energy block is reallocated to t_K. If the above two conditions are not satisfied, find the maximum of $e(t_2), \ldots, e(t_{K-1})$, and then reallocate the energy block to the time corresponding to the maximum.

The reallocating rules are both shown in Fig.6 with two different examples. After reallocating, the $P_i(t)$ for every load can be found, and then the $P_g(\cdot)$ is found. Then Algorithm 2 is finished.

After $P_g(\cdot)$ is obtained, the deviation between $P_{g,e}(t)$ and $P_g(t)$ in Algorithm 2 must be analyzed. The deviation appears in step three, reallocating. In step three, if $P_{g,e}(t)$ at a certain time appears in at least two energy blocks, it will have two part deviations, separately at the start and end of $P_{g,e}(t)$. According to Rule A and Rule B, the deviation of each part is no more than $0.5P_g^{rate}$, so the total deviation for $P_{g,e}(t)$ is no more than P_g^{rate}. For $P_{g,e}(t)$ appearing in only one energy block, there must be $P_{g,e}(t) \leq P_g^{rate}$. If the energy block is reallocated to time t, the deviation is $|P_g^{rate} - P_{g,e}(t)| \leq P_g^{rate}$; otherwise, the deviation is $|P_{g,e}(t) - 0| \leq P_g^{rate}$. Therefore, for any $P_{g,e}(t)$, the deviation between $P_{g,e}(t)$ and $P_g(t)$ is no more than P_g^{rate}.

Then the operability of $P_g(\cdot)$ obtained in Algorithm 2 needs to be verified. Here the counter-evidence method is used for analysis. If there is a certain time t, two energy blocks of $P_g(t)$ are allocated to a load i. Then for the $P_{g,e}(t)$ corresponding to $P_g(t)$, based on the allocation order in step two, each load except for load $i$has an energy block fully occupied by $P_{g,e}(t)$, which means N-1 energy blocks. Meanwhile, for two energy blocks of $P_g(t)$ that are allocated to load i, in the block of the left column, $P_{g,e}(t)$ must occupy no less than half of the block, and in the block of the right column, $P_{g,e}(t)$ must occupy more than half of the block. Add these energy blocks together, and then the whole $P_{g,e}(t)$ is larger than NP_g^{rate}, which is against the constraints for $P_{g,e}(t)$ in (20). Therefore, for any $P_g(t)$, its energy blocks cannot allocate more than one block to a load. $P_g(\cdot)$ is operational and $P_g(\cdot) \in \mathcal{P}_g$.

Through analysis of deviation and feasibility, a $P_g(\cdot)$ that fulfills (21) is found by Algorithm 2. Hence, Equation (21) and Theorem 3 are verified.

Theorem 3 establishes a continuous equivalent model for ON/OFF loads, which is approximate to a hydropower plant model. Although there are some deviations in the equivalent model, the deviations would be negligible if N is large enough. Besides, the equivalent model established is linear with continuous variables only, which makes it easy to add to optimization models without increasing their complexity.

D. GROUP MERGER

Through merging some of the groups with similar parameters, the number of groups is reduced, as well as the number of variables and constraints. Based on the above proof process, P_g^{rate} has the least impact on the proof. Therefore, the groups with different P_g^{rate} could be merged together into a larger group, in which the rate powers of loads are diverse. The equivalent model for continuous loads and ON/OFF loads

of the merged group is established based on Theorem 4 and Theorem 5, respectively.

Theorem 4: For a group of N continuous flexible loads with same parameters of α_g, β_g, T_g, and P_i^{rate} for any load i is a positive number as the parameter. If its model $\mathcal{P}_g$ is in the following form:

$$\mathcal{P}_g = \left\{ P_g(\cdot) \left| \begin{array}{c} P_g(t) = \sum_{i=1}^{N} P_i(t),\ \forall t \\ 0 \le P_i(t) \le P_i^{rate},\ \forall i,\ \forall t \\ P_i(t) = 0,\ t \notin [\alpha_g, \beta_g],\ \forall i \\ \sum_t P_i(t) = T_g P_i^{rate},\ \forall i \end{array} \right. \right\} \tag{24}$$

The model $\mathcal{P}_g$ could be equivalent to the model $\mathcal{P}_{g,e}$, whose form is as follows:

$$\mathcal{P}_{g,e} = \left\{ P_{g,e}(\cdot) \left| \begin{array}{c} 0 \le P_{g,e}(t) \le \sum_i P_i^{rate},\ \forall t \\ P_{g,e}(t) = 0,\ t \notin [\alpha_g, \beta_g] \\ \sum_t P_{g,e}(t) = \sum_i T_g P_i^{rate} \end{array} \right. \right\} \tag{25}$$

Proof: $\mathcal{P}_g$ being equivalent to the model $\mathcal{P}_{g,e}$ means that (16) and (17) are fulfilled. The proof for (16) is exactly the same as in Theorem 1. For (17), let every $P_i(t)$ equal to $P_{g,e}(t)P_i^{rate}/\sum_i P_i^{rate}$, and then it can be verified that Equation (17) is fulfilled. Hence Theorem 4 is verified.

Theorem 5: For a group of N ON/OFF flexible loads, parameters α_g, β_g, and T_g are the same, while the P_i^{rate} for load i can be different. If its model $\mathcal{P}_g$ is in the following form:

$$\mathcal{P}_g = \left\{ P_g(\cdot) \left| \begin{array}{c} P_g(t) = \sum_{i=1}^{N} P_i(t),\ \forall t \\ P_i(t) = u_i(t) P_i^{rate},\ \forall t,\ \forall i \\ u_i(t) \in \{0, 1\},\ \forall t,\ \forall i \\ P_i(t) = 0,\ t \notin [\alpha_g, \beta_g],\ \forall i \\ \sum_t P_i(t) = T_g P_i^{rate},\ \forall i \end{array} \right. \right\} \tag{26}$$

There is a model $\mathcal{P}_{g,e}$ that is ε-equivalent to $\mathcal{P}_g$, and in the ε-equivalence, the $\|\cdot\| = \|\cdot\|_\infty$ and $\varepsilon = \max(P_i^{rate})$. The form of $\mathcal{P}_{g,e}$ is as in (25).

Proof: $\mathcal{P}_g$ being equivalent to the model $\mathcal{P}_{g,e}$ means that (20) and (21) are fulfilled. The proof for (20) is the same as the proof in Theorem 3. To prove (21), for any $P_{g,e}(t)$ in $\mathcal{P}_{g,e}$, apply the proposed Algorithm 2, and then obtain the $P_i(t)$ for every load, as well as the $P_g(\cdot)$.

After $P_g(\cdot)$ is obtained, deviation analysis between $P_{g,e}(t)$ and $P_g(t)$ and operability analysis for $P_g(\cdot)$ are needed. Theorem 3 proves that if $P_{g,e}(t)$ appears in at least two energy blocks, it will have two parts of deviations, and the deviation of each part is no more than $0.5P_i^{rate}$. Due to $P_i^{rate} \le \max(P_i^{rate})$ for any load i, the total deviation for $P_{g,e}(t)$ is no more than $\max(P_i^{rate})$. For $P_{g,e}(t)$ appearing in only one energy block, Theorem 3 proves that the deviation is no more than the P_i^{rate}, therefore the deviation is no more than the $\max(P_i^{rate})$. Hence, for any $P_{g,e}(t)$, the deviation between $P_{g,e}(t)$ and $P_g(t)$ is no more than the $\max(P_i^{rate})$. The operability analysis for $P_g(\cdot)$ is the same as the analysis in Theorem 3. Theorem 5 is thus verified.

In Theorem 5, as long as the $\max(P_i^{rate})$ is not too large, the continuous equivalent model can significantly reduce the number of groups, and ensure a certain limit of equivalence deviations.

IV. SCHEDULING WITH EQUIVALENT AGGREGATED MODEL

The key to scheduling with the equivalent aggregated model is to reasonably group a set of flexible loads. There are two factors that should be considered for loads grouping, namely the distributions of load parameters and the scheduling requirements of the power system.

According to the Theorems in Section III, the equivalent model is established based on a group of loads with the same or similar parameters. Therefore, the distributions of load parameters are very important for grouping progress as well as the parameters of the equivalent model.

The requirements of system scheduling also need to be taken into account. In general, a flexible load may have a wide scheduling period, but after system scheduling, the load will only work in the valley of the system load [31]. Hence, the schedulable period outside the valley of the system load has little effect on scheduling of the load. Thus, when building a group, $[\alpha_g, \beta_g]$ of the group can be set in the valley of the system load, instead of over the whole schedulable period. A group built in this way will have a smaller schedulable period, which allows more loads to work in this period, and to be assigned to this group. Then, as each group becomes larger, the number of groups becomes smaller. Therefore, the specific range in which the flexible loads mainly work needs to be calculated as the Reference Scheduling Period used for grouping criteria.

In the rest of this Section, the process to calculate the Reference Scheduling Period is illustrated, along with the method to group flexible loads based on the Reference Scheduling Period and load parameters distributions. The approach to scheduling with the equivalent models of groups is also presented.

A. REFERENCE SCHEDULING PERIOD

In order to obtain a possible load-operating period as the Reference Scheduling Period, a relaxation model of the set of flexible loads is used for preliminary scheduling. Consider a set Ω of flexible loads in the form of (5-7), where α_i, β_i separately obey a probability distribution. The range of α_i is $[\alpha_{p1}, \alpha_{p2}]$, while the range of β_i is $[\beta_{p1}, \beta_{p2}]$. The relaxation model $\mathcal{P}_r$ of the set is described by (27):

$$\mathcal{P}_r = \left\{ P_r(\cdot) \left| \begin{array}{c} 0 \le P_r(t) \le \sum_i P_i^{rate},\ \forall t \\ P_r(t) = 0, \quad t \notin [\alpha_{p1}, \beta_{p2}] \\ \sum_t P_r(t) = \sum_i T_i P_i^{rate} \end{array} \right. \right\} \tag{27}$$

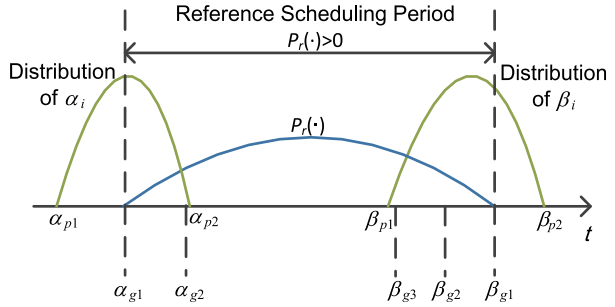

FIGURE 7. Decision grouping criteria based on Reference Scheduling Period.

Without a loss of generality, it's assumed that $\alpha_{p1} < \alpha_{p2}$, $\beta_{p1} < \beta_{p2}$, and $\alpha_{p1} < \beta_{p2}$; and if the domain of α_i or β_i includes $+\infty$ or $-\infty$, the quantiles can be used to obtain the range in which most of the probability is concentrated.

Consider a scheduling optimization with a set Ω of flexible loads as described by (28):

$$\min = F(\sum_{i\in\Omega} P_i(\cdot), Y), \quad s.t.\ Y \in \mathcal{Y},\ P_i(\cdot) \in \mathcal{P}_i,\ \forall i \quad (28)$$

where Y is the vector of other optimization variables in scheduling, and its feasible domain is $\mathcal{Y}$.

The sum of $P_i(\cdot)$ can be replaced with the relaxation model, as in (29):

$$\min = F(P_r(\cdot), Y), \quad s.t.\ Y \in \mathcal{Y},\ P_r(\cdot) \in \mathcal{P}_r \quad (29)$$

The scheduling optimization (29) can be solved by conventional algorithms because the relaxation model is a linear model, which does not increase complexity. After the $P_r(\cdot)$ is obtained, the period of $P_r(\cdot) > 0$ is the best operating time for flexible loads based on the scheduling. Usually, the period of $P_r(\cdot) > 0$ is a continuous interval in the valley of the system load, and can be used as the Reference Scheduling Period. However, if the period of $P_r(\cdot) > 0$ consists of a few discontinuous intervals, we can find a minimum continuous interval containing the period of $P_r(\cdot) > 0$, and then use it as the Reference Scheduling Period.

B. GROUPING

After obtaining the Reference Scheduling Period, grouping criteria and the parameters of groups need to be determined, and then the loads in set Ω can be grouped.

1) SETTING OF GROUPS

According to Section III, the key parameters for a group are α_g, β_g, and T_g. Hence the main goal of groups setting is to find the ranges of α_g, β_g, and T_g as the grouping criteria.

The range of T_g is made of the unique T_i values of all the loads; it consists of some discrete values. The method to decide the range of α_g, β_g is shown in Fig.7.

For the range of α_g, obtain the value from the start of the Reference Scheduling Period, then backward at regular intervals, until α_{p2}, the end of distribution of α_i. For the range of β_g, obtain the value from the end of Reference Scheduling Period, then forward at regular intervals, until β_{p1}, the start of distribution of β_i. With these rules, in Fig.7 the range of α_g is $\{\alpha_{g1}, \alpha_{g2}\}$, and the range of β_g is $\{\beta_{g1}, \beta_{g2}, \beta_{g3}\}$.

The parameters for groups can thus be set with the combination of the values in the ranges of α_g, β_g, and T_g. After setting groups, the group whose $T_g > \beta_g - \alpha_g + 1$ needs to be deleted, because these parameters will cause the internal loads to have insufficient time to complete their work. In addition, an Unclassified Group must be established to accommodate the loads that cannot be assigned to the above groups.

2) GROUPING LOADS

For each load i with α_i, β_i, and T_i in set Ω, if the parameters of the group it belongs to are $\alpha_{i,g}$, $\beta_{i,g}$, and $T_{i,g}$, then the following steps can be used for grouping:

① As for $\alpha_{i,g}$, it's the value that fulfills: $\alpha_{i,g} \in$ range of α_g, $\alpha_{i,g} \geq \alpha_i$, and $\alpha_{i,g}$ is as small as possible.
② As for $\beta_{i,g}$, it's the value that fulfills: $\beta_{i,g} \in$ range of β_g, $\beta_{i,g} \leq \beta_i$, and $\beta_{i,g}$ is as big as possible.
③ As for $T_{i,g}$, $T_{i,g} = T_i$.
④ If there is no $\alpha_{i,g}$ or $\beta_{i,g}$ or $T_{i,g}$ that fulfills the above conditions, the load i is assigned to the Unclassified Group. If $\alpha_{i,g}$, $\beta_{i,g}$ and $T_{i,g}$ all exist, find the group with the parameters of $\alpha_{i,g}$, $\beta_{i,g}$, $T_{i,g}$ in the groups that are set in Section IV.B. If the group exists, the load i is assigned to this group. Otherwise, the load i is assigned to the Unclassified Group.

$\alpha_{i,g} \geq \alpha_i$, and $\beta_{i,g} \leq \beta_i$ are used to ensure that the $[\alpha_{i,g}, \beta_{i,g}]$ is the subinterval of $[\alpha_i, \beta_i]$, so the load $i$can work in $[\alpha_{i,g}, \beta_{i,g}]$. The $[\alpha_{i,g}, \beta_{i,g}]$ should be as big as possible to maintain the flexibility of load i, so $\alpha_{i,g}$ should be small and $\beta_{i,g}$ should be big. Afterwards, the load is classified into one of the groups established in Section IV.B based on $\alpha_{i,g}$, $\beta_{i,g}$ and $T_{i,g}$, and the ungrouped loads are placed in the Unclassified Group.

After loads grouping, groups having only a few loads can be deleted to reduce the number of groups. A threshold can be set for deleting, and the group whose number of loads is less than the threshold can be deleted. The loads of deleted groups are assigned to the Unclassified Group.

C. OPTIMIZATION WITH GROUPS

After grouping, the loads in scheduling optimization can be replaced by equivalent models of groups. Through replacing, the scheduling optimization in (28) can be described as follows:

$$\min = F(\sum_{g=1}^{M} P_{g,e}(\cdot) + \sum_{i\in U} P_i(\cdot), Y) \quad (30)$$

$$s.t.\ Y \in \mathcal{Y}, \quad P_{g,e}(\cdot) \in \mathcal{P}_{g,e},\ \forall g,\ P_i(\cdot) \in \mathcal{P}_i,\ \forall i \in U \quad (31)$$

In order to further simplify the scheduling model, the loads in the Unclassified Group are scheduled first through a

TABLE 1. Distributions of flexible loads' parameters.

Parameters	Distributions
α_i	$N(18{:}30\text{ h}, (1\text{h})^2)$
β_i	$N(7{:}30\text{ h}, (1\text{h})^2)$
E_i	$N(21\text{ kW·h}, (3\text{ kW·h})^2)$
P_i^{rate}	$U(6\text{ kW}, 12\text{ kW})$

heuristic algorithm, and then the scheduling optimization is solved. Although the loads in the Unclassified Group occupy a very small part of the total flexible loads, they bring many more variables and constraints than the other groups, because these loads are described by individual models. Therefore, a heuristic algorithm is used to schedule these loads first, and then scheduling optimization is solved with the equivalent models of groups. Although the result of the heuristic algorithm may have some deviations from the optimal solution in the first step, the deviations can be largely eliminated when scheduling the equivalent models of groups in the next step. In this way, the heuristic algorithm can reduce the number of variables and constraints, and the optimality of the solution is guaranteed by scheduling with equivalent models.

The heuristic algorithm used in this paper places each load in the valley of the total load, because the electricity cost in the load valley is generally lower. First, the algorithm obtains the base load of the system without flexible loads by load forecast, as the initial total load. Then it takes a load i from the Unclassified Group, and sets its working time in the valley of the total load as well as in its schedulable period $[\alpha_i, \beta_i]$. Afterwards, the algorithm updates the total load by adding the power of load i. Then it takes the next load, set its working time and updates the total load. Repeat these steps until all the loads in the Unclassified Group are scheduled.

Afterwards, scheduling optimization with equivalent models can be solved by conventional algorithms, and the $P_{g,e}(\cdot)$ of each group is obtained. Then the $P_{g,e}(\cdot)$ is disaggregated to the $P_i(\cdot)$ of each load inside. Then the actual power of the group $P_g(\cdot)$ is calculated as the sum of $P_i(\cdot)$. Finally the actual value of objective function is calculated with the $P_i(\cdot)$ of every load.

V. SIMULATION RESULTS

In this study, a case of day-ahead scheduling for a power system with large-scale flexible loads is analyzed. The scheduling period is set as 24h and the duration of a time interval Δt = is 0.25h. The day-ahead load forecast of base load comes from historical data of the UK power system [32]. Then 1×10^6 electric vehicles that need to charge at night are considered as the flexible loads that participate in the day-ahead scheduling. These flexible loads work in ON/OFF mode, and make up the set Ω. The distributions of their parameters are shown in Table 1.

In Table 1, α_i, β_i, and E_i follow the Gaussian distribution and the P_i^{rate} follows the Uniform distribution. With parameters of E_i and P_i^{rate}, the T_i can be calculated and rounded to an integer.

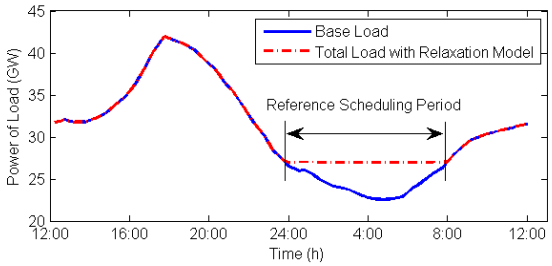

FIGURE 8. Total load after scheduling with relaxation model.

TABLE 2. Grouping criteria.

Criteria	Value
Range of α_g	{23:45}
Range of β_g	{ 7:45 , 7:15, 6:45, 6:15, 5:45, 5:15, 4:45}
Range of T_g	{4,5,…, 21,22}

In terms of power supply, a quadratic function is used to express the total cost of the system's power supply [33]:

$$C = \sum_{t=1}^{T} (aP_{total}(t)^2 + bP_{total}(t) + c) \tag{32}$$

where $P_{total}(t)$ is the total load of the power system (MW), and $a = 2 \times 10^{-4}$ £/MW^2, $b = 0.3$ £/MW, $c = 15000$ £. The goal of day-ahead scheduling is to minimize the total cost of the power supply by scheduling flexible loads. All calculations are completed in MATLAB 2014a, on a computer with Intel i7 8750H and 16G RAM.

A. RESULT OF SCHEDULING

This section presents the process of scheduling with the equivalent aggregated model, and compares its scheduling result with two other scenarios.

In order to schedule with the equivalent aggregated model, first the Reference Scheduling Period needs to be calculated. Since the relaxation model needs to cover almost all of the loads, its schedulable period is set as [15:30, 10:30], based on the 3σ criterion. Its upper limit of rate power is the sum of the P_i^{rate} of all flexible loads, and its energy is the sum of the $T_i P_i^{rate} \Delta t$ of all the loads. Solve day-ahead scheduling with the relaxation model, and then a relaxed solution $P_r(\cdot)$ can be obtained as Fig.8 shows.

The time for $P_r(\cdot) > 0$ is [23:45, 7:45], which is the Reference Scheduling Period. Afterwards, the grouping criteria are established based on the Reference Scheduling Period, as shown in Table 2.

Because almost every $\alpha_i \leq 23{:}45$, the range of α_g, as the start of the schedulable period for all the groups is 23:45. However, because distribution for β_i intersects with the Reference Scheduling Period, the range of β_g, as the end of the schedulable period for groups, starts from 7:45 and ends at 4:45, for more than 99% $\beta_i \geq 4{:}45$. The time interval in the range of β_g is set as $2\Delta t$ to reduce numbers of groups. The range of T_g consists of the unique values of T_i.

TABLE 3. Parameters of some groups.

Index	α_g	β_g	T_g	Number of Loads	$\sum P_i^{rate}$ (MW)
1	23:45	7:45	5	1137	12.72
2	23:45	7:45	6	8594	95.19
3	23:45	7:45	7	30711	334.10
4	23:45	7:45	8	55268	579.21
5	23:45	7:45	9	61839	608.80
…	…	…	…	…	…
31	23:45	6:45	8	28957	303.43
32	23:45	6:45	9	32094	316.62
33	23:45	6:45	10	28120	253.89
34	23:45	6:45	11	22738	187.69
35	23:45	6:45	12	18107	138.34
…	…	…	…	…	…
51	23:45	6:15	16	2136	13.84
52	23:45	6:15	17	945	6.01
53	23:45	5:45	6	1836	20.38
54	23:45	5:45	7	6622	72.05
55	23:45	5:45	8	12402	130.01
…	…	…	…	…	…
81	23:45	4:45	12	1185	9.05
82	23:45	4:45	13	893	6.40
83	23:45	4:45	14	610	4.17

There are thus 133 groups initially, with an Unclassified Group, and then the flexible loads are assigned into the groups. In this case, the threshold for deleting the group is 0.05% of the number of flexible loads. After grouping, 83 groups are obtained, and they cover 991,029 flexible loads, leaving 8,971 flexible loads in the Unclassified Group. The parameters of some groups are listed in Table 3.

After grouping, a heuristic algorithm is applied to loads in the Unclassified Group, and then conventional algorithms can solve scheduling with equivalent models of groups. Then the $P_i(\cdot)$ of each load and the $P_g(\cdot)$ of each group are obtained based on Theorem 5, and the power of the total load is also acquired.

The result of scheduling with an equivalent aggregated model is compared with the following two scenarios:

Scenario 1: Early finish. In this scenario, all the loads will start working at the start of their schedulable period, and work continuously until their works are completed. Hence all the loads finish their work as early as possible.

Scenario 2: Independent scheduling. In this scenario, the system operator broadcasts an electricity price to all the flexible loads, and the electricity price is positively related to the forecast of the base load. Then each load is scheduled independently to minimize its own electricity costs.

Fig.9 shows the total load of the system in different scenarios.

Scenario 1 reflects the natural energy demand of the flexible loads. Each load finishes its work as early as possible, which is most beneficial to the user's need. However, the scheduling mode leads the flexible loads to be superimposed on the peak period of the base load, and results in an increase in peak load. The scheduling result will not only increase the total cost of the power system, but also propose higher requirements on the generation capacity of the system.

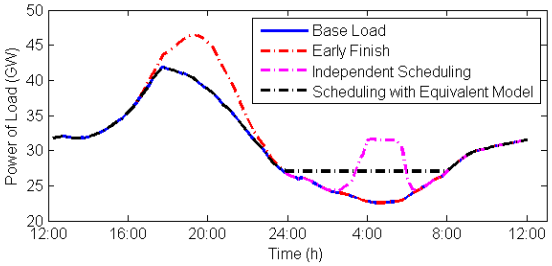

FIGURE 9. Total load in different scenarios of scheduling.

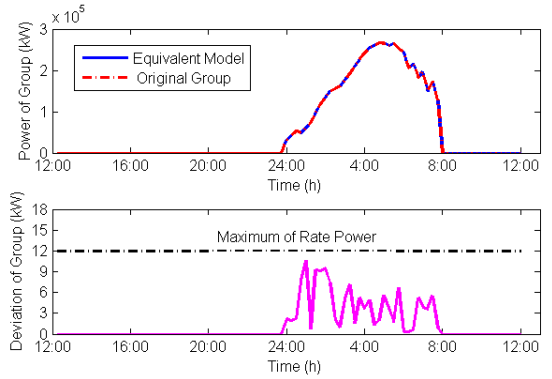

FIGURE 10. Power and deviation of the group with most loads.

Scenario 2 represents the operation of flexible loads under non-cooperative independent scheduling. Each flexible load will independently schedule its operation to minimize its cost, according to the electricity price from the system operator. All loads would work at the valley of the electricity price, and as a result, form a load peak at the valley. The problem is hard to solve by adjusting electricity prices. Regardless of how the electricity price is set, as long as the prices received by all flexible loads are the same, their responses will be similar, and the loads will be concentrated at the valley of the electricity price, where a peak load will be formed. The way to solve the problem is coordinated scheduling. Scheduling with the equivalent aggregated model described in this paper is an approach to coordinated load scheduling. In Fig.9, a scheduling model coordinates the flexible loads well, and the valley of the total load is almost filled into a horizontal line by flexible loads. It illustrates that the proposed equivalent aggregated model is effective in a scheduling model.

B. DEVIATIONS OF EQUIVALENCE

This section analyzes the equivalence deviation of each group. The equivalence deviation is the deviation between $P_g(\cdot)$ of the original group and $P_{g,e}(\cdot)$ of its equivalent model. Theorem 5 draws a conclusion that, for a group of ON/OFF loads, the deviation between $P_g(\cdot)$ and $P_{g,e}(\cdot)$ will not exceed the maximum rated power of the loads at any time. Therefore, the equivalence deviation of each group is calculated to verify that conclusion.

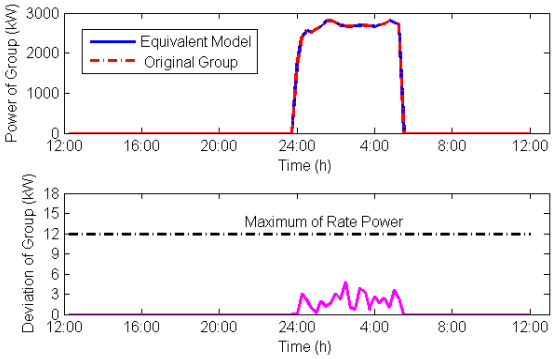

FIGURE 11. Power and deviation of the group with least loads.

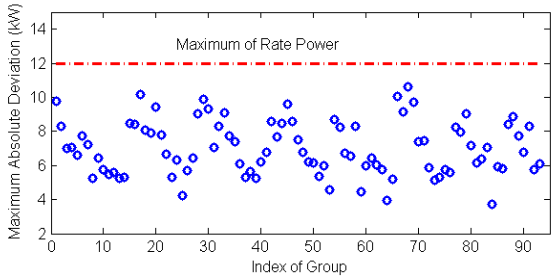

FIGURE 12. Maximum absolute deviation of all groups.

Groups with the most loads and the least loads are analyzed as examples, and their load curves and the absolute deviation $|P_{g,e}(\cdot)-P_g(\cdot)|$ are shown in Fig.10 and Fig.11. It can be seen that the $P_{g,e}(\cdot)$ of the equivalent model is almost coincident with the $P_g(\cdot)$ of the original group. This indicates that the equivalent model and the original group are highly consistent in the characteristics of the total power. Then, regardless of the number of loads in the group, the absolute deviation between $P_{g,e}(\cdot)$ and $P_g(\cdot)$ does not exceed the maximum rated power, 12 kW at any time, which verifies the conclusion of Theorem 5. Considering the total power of a group is in the range of several MW to hundred MW, the absolute deviation of 12 kW is almost negligible, which indicates the high accuracy of the equivalent model. Finally, the deviation of the groups only occurs when $P_{g,e}(t) \neq 0$, which is consistent with the proving process in Section III. This is because the $P_{g,e}(t)$ equal to 0 does not participate in the power disaggregation process, so when $P_{g,e}(t) = 0$, the corresponding $P_g(t) = 0$, and the deviation is thus 0.

In order to display the deviation of all groups, the maximum absolute deviation at all times, $\|P_{g,e}(\cdot) - P_g(\cdot)\|_\infty$, is calculated and shown in Fig.12. It's clear that the maximum absolute deviations of all groups do not exceed 12 kW, the maximum rated power of the loads. Hence, the result verifies the conclusion of Theorem 5.

The total power of all groups $\sum P_g(\cdot)$, the total power of all equivalent models $\sum P_{g,e}(\cdot)$, and their absolute deviation are shown in Fig.13. The $\sum P_g(\cdot)$ of all equivalent models is almost coincident with the $\sum P_{g,e}(\cdot)$ of all groups, which indicates that the equivalent models are

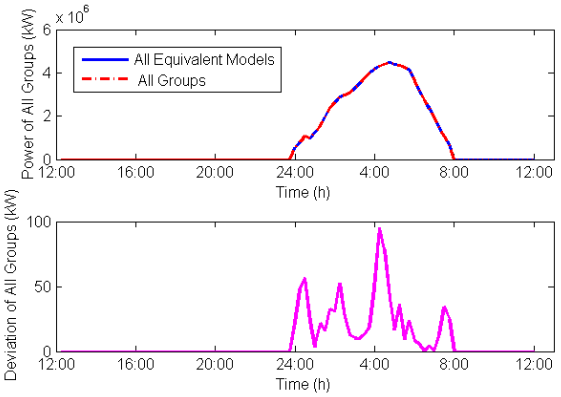

FIGURE 13. Power and deviation of all groups.

highly accurate. Then, according to Theorem 5, the upper limit of the total deviation can be estimated. Since the upper limit of the deviation of each group is $\max(P_i^{rate})$, or 12 kW, the upper limit of the total deviation is the $\max(P_i^{rate})$ multiplied by the number of groups, or 996 kW. However, since the deviations in disaggregation progress are random, the positive and negative equivalence deviations from different groups will cancel each other out, so the actual total deviation of all groups can be much smaller than 996 kW. In this case, the actual total deviation is no more than 100 kW, which is consistent with our estimation. Considering the total power of all groups is up to several GW, the total deviation of 100 kW is almost negligible. The $P_i(\cdot)$ of each flexible load has been verified to meet its constraints, illustrating that the result for each load is operational.

C. CALCULATION PERFORMANCE

This section analyzes the calculation performance of the equivalence algorithm, which schedules with the equivalent aggregated model, and compares it with the distributed algorithm in [15]. The distributed algorithm sequentially schedules the working time of the load, and repeatedly iterates until the scheduling model converges. Reference [15] applied the distributed algorithm to large-scale flexible loads scheduling and carried out a case study; hence it serves as a comparison algorithm for this paper. Flexible loads schedules of two algorithms are $P_{\Omega,eq}(\cdot)$ and $P_{\Omega,dis}(\cdot)$, and their deviation is measured by maximum absolute deviation, $\|P_{\Omega,eq}(\cdot)$-$P_{\Omega,dis}(\cdot)\|_\infty$. The equivalence algorithm and the distributed algorithm are tested on the same hardware and software platform, and in the step of optimization with equivalent models, YALMIP/IPOPT is used as the optimization tool. Other steps are implemented by MATLAB code.

Table 4 displays the calculation time for the two algorithms to schedule one million flexible loads. The calculation time of each step in the equivalence algorithm is described separately. Overall, the calculation speed of the equivalence algorithm is nearly 154 times faster than the distributed algorithm, and its calculation efficiency increases by more than two-orders of magnitude. The most time-consuming step of the equivalence

TABLE 4. Calculation time of two algorithms with one million loads.

Criteria	Time(s)	
	Equivalence Algorithm	Distributed Algorithm
Reference Scheduling Period	0.51	
Grouping	8.07	
Heuristic Algorithm for Other Group	0.66	\
Optimization with Groups	0.99	
Group Power Disaggregated	1.580	
Total	11.81	1829.44

TABLE 5. Calculation time and scheduling results of two algorithms under different scales of loads.

Number of Loads	Equivalence Algorithm		Distributed Algorithm		Maximum Absolute Deviation (kW)
	Time (s)	Total cost ($\times 10^7$£)	Time (s)	Total cost ($\times 10^7$£)	
100,000	2.08	2.100	178.81	2.100	122.51
250,000	3.43	2.113	479.00	2.113	47.35
500,000	6.14	2.136	981.93	2.136	47.31
750,000	8.92	2.160	1364.81	2.160	61.62
1,000,000	11.81	2.184	1829.44	2.184	95.69
1,250,000	14.12	2.209	2361.04	2.209	119.43
1,500,000	17.23	2.234	2890.91	2.234	70.51
1,750,000	20.05	2.260	3664.67	2.260	70.12
2,000,000	23.09	2.287	4994.24	2.287	72.74

algorithm is grouping, which accounts for 68% of the time used by the entire algorithm. The reason for the time-consuming step is that a large number of loop calculations are required to group each load. However, since the process of load grouping is independent, the step of grouping can be accelerated by parallel computing. Afterwards, the key step of scheduling, optimization with groups is solved in about one second. The reason that this step can be solved so quickly is that a large number of loads with discrete variables are equivalent to the equivalent load models with continuous variables and linear constraints, which makes it possible to use conventional algorithms and existing solvers, and hence the model is solved efficiently. By contrast, the distributed algorithm needs to repeatedly iterate all the loads in sequence, and the iterative process for the loads is performed serially, which results in a relatively slow solving speed.

Table 5 displays the calculation time and scheduling results of the two algorithms under different scales of loads. Under different scales of flexible loads, the proposed equivalence algorithm achieves the same total cost of the system as the distributed algorithm, and the deviation between flexible loads schedules is also very small. However, the equivalence algorithm performs scheduling in just tens of seconds, which is much faster than the distributed algorithm. The equivalence algorithm's calculation time is nearly linear with the numbers of loads, which means that the algorithm has good scalability for large-scale load scheduling. During the process of scheduling, the step of grouping often takes up more than 60% of the total calculation time, whereas the other steps just take a few seconds. The step of grouping can be accelerated by parallel computing, so the time consumption of the equivalence algorithm can be further reduced, which is quite useful for scheduling with a large number of flexible loads. In addition, since the equivalent model of the group is linear and continuous, it can be easily embedded in various scheduling models without increasing their complexity, which is also difficult for the distributed algorithm to accomplish.

VI. CONCLUSION

With the rapid development of smart grid technology, large-scale flexible loads are being integrated into the bulk power system, posing a great challenge for system operation. Focusing on the scheduling of the power system with large-scale flexible loads, this paper proposes an equivalent aggregated model of flexible loads based on grouping equivalence, proves the equivalence between the models, estimates the upper bound of equivalent deviations, and establishes a scheduling model applying the equivalent aggregated model.

The case study indicates that the proposed model can be effective in the scheduling of large-scale flexible loads, which makes the loads operate coordinately at the system valley instead of causing a load peak. The deviation between the equivalent model and the original group is quite small, which indicates that the equivalent model is highly accurate. When compared with the distributed algorithm, the equivalence algorithm based on the equivalent aggregated model can optimize the scheduling of large-scale flexible loads in a short time, which is faster by two orders of magnitude than the distributed algorithm. Overall, the equivalent aggregated model and the related scheduling method provide an effective solution for large-scale flexible loads to participate in power system scheduling. The fast calculation of the equivalent aggregated model makes it promising for day-ahead, intraday and real-time scheduling.

REFERENCES

[1] P. Y. Kong and G. K. Karagiannidis, "Charging schemes for plug-in hybrid electric vehicles in smart grid: A survey," *IEEE Access*, vol. 4, pp. 6846–6875, Nov. 2016.

[2] H. Shareef, M. S. Ahmed, A. Mohamed, and E. A. Hassan, "Review on home energy management system considering demand responses, smart technologies, and intelligent controllers," *IEEE Access*, vol. 6, pp. 24498–24509, 2018.

[3] S. Chandrashekar, Y. Liu, and R. Sioshansi, "Wind-integration benefits of controlled plug-in electric vehicle charging," *J. Mod. Power Syst. Clean Energy*, vol. 5, no. 5, pp. 746–756, Sep. 2017.

[4] Q. Shi, F. Li, G. Liu, D. Shi, Z. Yi, and Z. Wang, "Thermostatic load control for system frequency regulation considering daily demand profile and progressive recovery," *IEEE Trans. Smart Grid*, to be published.

[5] Q. Shi, F. Li, Q. Hu, and Z. Wang, "Dynamic demand control for system frequency regulation: Concept review, algorithm comparison, and future vision," *Electr. Power Syst. Res.*, vol. 154, pp. 75–87, Jan. 2018.

[6] V. Trovato, I. M. Sanz, B. Chaudhuri, and G. Strbac, "Advanced control of thermostatic loads for rapid frequency response in Great Britain," *IEEE Trans. Power Syst.*, vol. 32, no. 3, pp. 2106–2117, May 2017.

[7] Y. Ding, W. Cui, S. Zhang, H. Hui, Y. Qiu, and Y. Song, "Multi-state operating reserve model of aggregate thermostatically-controlled-loads for power system short-term reliability evaluation," *Appl. Energy*, vol. 241, pp. 46–58, May 2019.

[8] P. Liu and J. Yu, "Identification of charging behavior characteristic for large-scale heterogeneous electric vehicle fleet," *J. Mod. Power Syst. Clean Energy*, vol. 6, no. 3, pp. 567–581, May 2018.
[9] Y. Li, Z. Yang, D. Zhao, H. Lei, B. Cui, and S. Li, "Incorporating energy storage and user experience in isolated microgrid dispatch using a multi-objective model," *IET Renew. Power Gener.*, vol. 13, no. 6, pp. 973–981, Apr. 2019.
[10] H. Xia, Q. Li, R. Xu, T. Chen, J. Wang, and Muhamma, "Distributed control method for economic dispatch in islanded microgrids with renewable energy sources," *IEEE Access*, vol. 6, pp. 21802–21811, Apr. 2018.
[11] S. G. M. Rokni, M. Radmehr, and A. Zakariazadeh, "Optimum energy resource scheduling in a microgrid using a distributed algorithm framework," *Sustain. Cities Soc.*, vol. 37, pp. 222–231, Feb. 2018.
[12] J. Rivera, C. Goebel, and H.-A. Jacobsen, "Distributed convex optimization for electric vehicle aggregators," *IEEE Trans. Smart Grid*, vol. 8, no. 4, pp. 1852–1863, Jul. 2017.
[13] H. Fan, C. Duan, C. Zhang, L. Jiang, C. Mao, and D. Wang, "ADMM-based multiperiod optimal power flow considering plug-in electric vehicles charging," *IEEE Trans. Power Syst.*, vol. 33, no. 4, pp. 3886–3897, Jul. 2018.
[14] A.-H. Mohsenian-Rad, V. W. S. Wong, J. Jatskevich, R. Schober, and A. Leon-Garcia, "Autonomous demand-side management based on game-theoretic energy consumption scheduling for the future smart grid," *IEEE Trans. Smart Grid*, vol. 1, no. 3, pp. 320–331, Dec. 2010.
[15] A. De Paola, D. Angeli, and G. Strbac, "Price-based schemes for distributed coordination of flexible demand in the electricity market," *IEEE Trans. Smart Grid*, vol. 8, no. 6, pp. 3104–3116, Nov. 2017.
[16] M. Kumar, V. Gupta, R. Kumar, and B. K. Panigrahi, "Customer oriented electric vehicle charging scheduling in day-ahead market via aggregative game model," in *Proc. 8th IEEE India Int. Conf. Power Electron. (IICPE)*, Jaipur, India, Dec. 2018, pp. 1–6.
[17] S. Chen and R. S. Cheng, "Operating reserves provision from residential users through load aggregators in smart grid: A game theoretic approach," *IEEE Trans. Smart Grid*, vol. 10, no. 2, pp. 1588–1598, Mar. 2019.
[18] M. H. Yaghmaee, A. Leon-Garcia, and M. Moghaddassian, "On the performance of distributed and cloud-based demand response in smart grid," *IEEE Trans. Smart Grid*, vol. 9, no. 5, pp. 5403–5417, Sep. 2018.
[19] C. Yang and W. Lou, "On optimizing demand response management performance for microgrids under communication unreliability constraint," in *Proc. IEEE Global Commun. Conf. (GLOBECOM)*, San Diego, CA, USA, Dec. 2015, pp. 1–6.
[20] J. Zhao, C. Wan, Z. Xu, and J. Wang, "Risk-based day-ahead scheduling of electric vehicle aggregator using information gap decision theory," *IEEE Trans. Smart Grid*, vol. 8, no. 4, pp. 1609–1618, Jul. 2017.
[21] H. Cui, F. Li, X. Fang, H. Chen, and H. Wang, "Bilevel arbitrage potential evaluation for grid-scale energy storage considering wind power and LMP smoothing effect," *IEEE Trans. Sustain. Energy*, vol. 9, no. 2, pp. 707–718, Apr. 2018.
[22] D. Li, J. Wu, K. Shi, T. Ma, Y. Zhang, and R. Zhang, "Bi-level optimal dispatch model for micro energy grid based on load aggregator business," in *Proc. IEEE Conf. Energy Internet Energy Syst. Integr. (EI2)*, Beijing, China, Nov. 2017, pp. 1–6.
[23] Y. Li, Z. Yang, G. Li, Y. Mu, D. Zhao, C. Chen, and B. Shen, "Optimal scheduling of isolated microgrid with an electric vehicle battery swapping station in multi-stakeholder scenarios: A bi-level programming approach via real-time pricing," *Appl. Energy*, vol. 232, pp. 54–68, Dec. 2018.
[24] D. Wang, X. Guan, J. Wu, P. Li, P. Zan, and H. Xu, "Integrated energy exchange scheduling for multimicrogrid system with electric vehicles," *IEEE Trans. Smart Grid*, vol. 7, no. 4, pp. 1762–1774, Jul. 2016.
[25] S. U. Khan, K. K. Mehmood, Z. M. Haider, M. K. Rafique, and C.-H. Kim, "A bi-level EV aggregator coordination scheme for load variance minimization with renewable energy penetration adaptability," *Energies*, vol. 11, no. 10, p. 2809, Oct. 2018.
[26] L. Chen, X. Huang, H. Zhang, and Y. Luo, "A study on coordinated optimization of electric vehicle charging and charging pile selection," *Energies*, vol. 11, no. 6, p. 1350, May 2018.
[27] R. Shi, C. Sun, Z. Zhou, L. Zhang, and Z. Liang, "A robust economic dispatch of residential microgrid with wind power and electric vehicle integration," in *Proc. Chin. Control Decis. Conf. (CCDC)*, Yinchuan, China, May 2016, pp. 3672–3676.
[28] Y. Huang, C. Guo, L. Wang, Y. Bao, S. Dai, and Q. Ding, "A cluster-based dispatch strategy for electric vehicles considering user satisfaction," *Autom. Electr. Power Syst.*, vol. 39, no. 17, pp. 183–191, Sep. 2015.
[29] Z. Pan, X. Zhang, T. Yu, and D. Wang, "Hierarchical real-time optimized dispatching for large-scale clusters of electric vehicles," *Autom. Electr. Power Syst.*, vol. 41, no. 16, pp. 96–104, Aug. 2017.
[30] J.-M. Clairand, J. Rodríguez-García, and C. Álvarez-Bel, "Smart charging for electric vehicle aggregators considering users' preferences," *IEEE Access*, vol. 6, pp. 54624–54635, 2018.
[31] S. Bahrami, M. H. Amini, M. Shafie-Khah, and J. P. S. Cataláo, "A decentralized electricity market scheme enabling demand response deployment," *IEEE Trans. Power Syst.*, vol. 33, no. 4, pp. 4218–4227, Jul. 2018.
[32] National Grid ESO. *Historical Demand Data*. Accessed: Jun. 20, 2019. [Online]. Available: https://demandforecast.nationalgrid.com/efs_demand_forecast/faces/DataExplorer
[33] Z. Liu, Q. Wu, S. Huang, L. Wang, M. Shahidehpour, and Y. Xue, "Optimal day-ahead charging scheduling of electric vehicles through an aggregative game model," *IEEE Trans. Smart Grid*, vol. 9, no. 5, pp. 5173–5184, Sep. 2018.

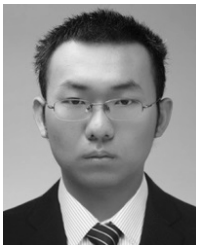

JING TU (S'19) was born in China. He received the B.S. degree in electrical engineering with its automation from North China Electricity Power University, Beijing, China, in 2014, where he is currently pursuing the Ph.D. degree in electrical engineering.

He is currently performing a research at the Department of Electrical Engineering and Computer Science, The University of Tennessee, Knoxville, TN, USA, as a Visiting Student. His main research interests include power system operation, demand response, and machine learning.

MING ZHOU (M'06) was born in China. She received the B.S., M.S., and Ph.D. degrees in electrical engineering from North China Electricity Power University, Beijing, China, in 1989, 1992, and 2006, respectively.

Since 1992, she has been with the School of Electrical and Electronic Engineering, North China Electricity Power University, where she is currently a Professor. Her research interests include power system economics, power system analysis and reliability, and power quality analysis.

HANTAO CUI (M'18) received the B.S. and M.S. degrees from Southeast University, China, in 2011 and 2013, respectively, and the Ph.D. degree from The University of Tennessee, Knoxville, in 2018, where he is currently a Research Assistant Professor with the Department of Electrical Engineering and Computer Science.

His research interests include large-scale power system simulations and cyber-physical systems.

FANGXING LI (FRANLI) (S'98–M'01–SM'05–F'17) received the B.S.E.E. and M.S.E.E. degrees from Southeast University, Nanjing, China, in 1994 and 1997, respectively, and the Ph.D. degree from Virginia Polytechnic Institute and State University, Blacksburg, VA, USA, in 2001.

He is currently a James McConnell Professor with The University of Tennessee (UT), Knoxville, TN, USA. His research interests include renewable energy integration, demand response, power markets, power system control, and power system computing.